Printed ISSN 1330–0008
Online ISSN 1333–9125
CD ISSN 1333–8390
CODEN FIZAE4

TEMPERATURE DEPENDENCE OF MICROSTRUCTURE OF $(1-x)$Al–xZn ALLOYS, $x = 0.44$, 0.48, 0.54 AND 0.62

ŽELJKO SKOKO and STANKO POPOVIĆ

Physics Department, Faculty of Science, University of Zagreb, Bijenička cesta 32, HR-10002 Zagreb, P.O. Box 331, Croatia
E-mail address: zskoko@phy.hr, spopovic@phy.hr

Dedicated to the memory of Professor Zvonko Ogorelec

Received 21 January 2005; Revised manuscript received 13 October 2005
Accepted 17 October 2005 Online 10 November 2006

The change of microstructure with temperature of the title alloys has been studied *in situ* by X-ray powder diffraction. It has been found that the temperature dependence of microstructure of the alloys, rapidly quenched from the solid-solution temperature, T_{ss}, to room temperature, RT, is quite different from that of the alloys slowly cooled from T_{ss} to RT. The area between two curves showing that dependence for the given phase during the first heating from RT to T_{ss} and first cooling from T_{ss} to RT is much smaller for the slowly-cooled alloys than for the rapidly quenched alloys. That area slightly increases with the increase of the Zn content in the alloys. The temperature dependence of microstructure of the alloys during the second heating from RT to T_{ss} and second cooling from T_{ss} to RT differs little from that during the first cooling from T_{ss} to RT. The ideal equilibrium state cannot be reached either by slow cooling of the alloys from T_{ss} to RT, or by a prolonged ageing at RT of the rapidly quenched alloys. The observed sequence of phase transitions in alloys during heating from RT to T_{ss} is different from that which could be expected according to the phase diagram of the system Al–Zn accepted in the literature. During cooling from T_{ss} to RT, a temperature hysteresis is observed in reversal phase transitions.

PACS numbers: 61.50.-f, 64.70, 64.75.-p, 64.75.+g, 65.70.+y UDC 548.73

Keywords: Al–Zn alloys, microstructure, phase transition, solid solution, X-ray powder diffraction

1. Introduction

The system Al–Zn is very suitable for studying phase transitions and microstructure for different compositions and/or temperatures. Zinc atoms do not form intermetallic phases with aluminium atoms due to a weak mutual interaction. The atomic radius of Al atoms is 0.143 nm, while the atomic radius of Zn atoms is 0.134

nm. This difference has a great influence on the microstructure of Al–Zn alloys. An Al–Zn alloy can gradually (asymptotically) approach the equilibrium state after a prolonged ageing at, say, room temperature (RT). This process can be accelerated at an elevated temperature, say, several tens K's above RT. In such a state, the alloy contains two phases: α-phase (fcc, the matrix, M) having ≈ 99 at % Al, and β(Zn)-phase (hexagonal, the precipitates) having ≈ 99.5 at % Zn. One can denote the α-phase in equilibrium with the phase β(Zn) as α(M/β).

The solubility of Zn in Al increases with temperature and reaches about 67 at % at 655 K [1]. The Al–Zn alloy rapidly quenched from the solid-solution temperature, T_{ss}, to RT is supersaturated and its decomposition takes place immediately after quenching. The sequence of precipitates appearing during a prolonged ageing is as follows: spherical Guinier–Preston zones (GPZ, fcc, coherent with M, having the diameter up to 3 to 4 nm, containing about 70 at % Zn) – ellipsoidal GPZ (fcc, coherent with M) – rhombohedrally distorted α'_R-phase (partially coherent with M, having particles of about ten nanometers in size) – metastable α'–phase (fcc, partially coherent with M) – β(Zn)-phase (incoherent with M, the final equilibrium precipitates having micrometer sizes). This sequence of phase transitions from one to the next type of precipitates depends on the initial composition of the alloy and on the thermal treatment [1].

The equilibrium phase diagram of the system Al–Zn has been defined on the basis of a number of articles and accepted in the literature [1,2].

In spite of many published data on the Al–Zn system, a systematic study of the system by X-ray powder diffraction (XRD), lacking in the literature, has been undertaken. A series of Al–Zn alloys having the Zn fraction $x = 0.045$, 0.08, 0.15, 0.20, 0.24, 0.26, 0.35, 0.38, 0.40, 0.44, 0.48, 0.54 and 0.62, prepared from components of purity 4N, were subjected to different thermal treatments. The alloys of different composition, quenched rapidly from T_{ss} to RT, were aged at RT or at elevated temperature, and the precipitation processes, that is, the decomposition of the supersaturated solid solutions, were followed during ageing. Also, the alloys of different composition, aged after quenching for different time intervals, were subjected to a gradual change of temperature, from RT to T_{ss} and back to RT, and their microstructure was followed *in situ* by XRD [3 – 6].

During the decomposition of the supersaturated alloy, a gradual transition of the solid solution, α_{ss}, to the equilibrium phase, α(M/β), takes place. That is clearly manifested in X-ray diffraction patterns because of different unit-cell parameters of the two phases, due to different content of Zn [3]. As various precipitates, P, grow inside the matrix, M, they cause strains in the crystal lattice of the matrix. X-ray diffraction lines of the matrix, α(M/P), are broader than those of pure Al [3]. Also, for the alloys approaching the equilibrium state, diffraction lines of the α(M/β)-phase are little broader than the ones of pure Al, because of strains in the matrix crystal lattice around the β(Zn) precipitates. On the other hand, diffraction lines of β(Zn) precipitates are rather sharp almost from the beginning of their appearance, indicating an unstrained crystal lattice [3].

GPZ are formed after quenching in alloys having $x \leq 0.48$. In the alloys with a higher Zn fraction, the decomposition process is rather fast and the sequence of precipitates is shortened [3]. The decomposition rate of the supersaturated alloy depends on the quenched-in vacancies (i.e. on the quenching rate), on the initial Zn fraction and the ageing temperature. It is the ageing temperature which strongly influences the diffusion rate of the Zn atoms inside the host Al crystal lattice (the matrix) [1,3].

These XRD studies have shown that accurate measurements of positions and profiles of diffraction lines yield useful information, e.g. on the zinc content in the matrix, M, for different precipitates, P, on the strains occurring at the M/P interface, on the unit-cell parameter of the intermediate phase, α', and of the solid solution, α_{ss}. Also, the recent investigations have shown that a correction of the phase diagram is necessary.

The present work is focused on the XRD study of the temperature dependence of microstructure of four Al–Zn alloys, with a high Zn fraction, $x = 0.44$, 0.48, 0.54, 0.62. The results obtained in this work are discussed in connection with two previous articles [5, 6]. That is, the present work is a review of a recent XRD study of the Al–Zn alloys, with the aim to check the validity of the phase diagram of the Al–Zn system in its central part, where the fractions of Al and Zn are comparable.

2. *Experimental*

The powder samples for XRD were prepared by filing the bulk alloys produced from elements of purity 4N. The samples were annealed up to 2 hours in the region of the solid-solution temperature, T_{ss} (up to 770 K), and quenched in water at RT. The samples were wrapped in a thin Al foil, perforated with hundreds of small holes in order to increase the quenching rate, which was estimated to 10^5 K/s. The quenching technique is described in detail in previous articles, e.g. Ref. [4].

The as-quenched alloys, having $x = 0.54$ and 0.62, being in a supersaturated state, were subjected to a prolonged ageing at RT. Having approached the equilibrium state, the alloys were studied by XRD. These samples were denoted as “water-quenched” and “prolonged” aged, in which “Zn is dominant”, WQZP.

The alloys having $x = 0.44$ and 0.48 were also rapidly quenched from T_{ss} in water at RT and then aged at RT for one week (the alloy with $x = 0.48$) or for two weeks (the alloy with $x = 0.44$), and for 11 months (both alloys, with $x = 0.44$ and 0.48). The samples aged at RT for one/two week(s) were denoted as “water-quenched” samples, in which “Al is dominant”, WQA. The samples aged at RT for 11 months were denoted as “water-quenched” and “prolonged” aged samples, in which “Al is dominant” WQAP. The alloys with $x = 0.44$ and 0.48 were also slowly cooled from T_{ss} to RT over 5 days, and then aged at RT for one week (the alloy with $x = 0.48$) or for two weeks (the alloy with $x = 0.44$). These alloys were denoted as “slowly-cooled” samples in which “Al is dominant”, SCA.

All samples, being quenched/slowly cooled from T_{ss} to RT and then aged at RT, tended to the equilibrium state. One may suppose that, after ageing at RT, the SCA samples were closer to the equilibrium state than the WQA samples. We wanted to find out whether the quenching from T_{ss} to RT and prolonged ageing at RT for 11 months produced a similar effect as slow cooling from T_{ss} to RT and short ageing at RT, that is, which samples, WQAP or SCA, were closer to the equilibrium state. It was also of interest to compare samples in which Zn is dominant, WQZP, with those in which Al is dominant, WQA and WQAP.

After ageing at RT, the samples were studied by XRD using a Philips diffractometer, having a high-temperature attachment (proportional counter, graphite monochromator, radiation Cu$K\alpha$). The samples were heated (by a platinum strip) from RT to T_{ss} and then cooled to RT, at a rate of 2 to 3 K/min. The heating/cooling of samples was stopped at a series of selected temperatures (20 to 30) for 15 minutes in order to scan prominent diffraction line profiles. In some cases, two heating and cooling cycles, between RT and T_{ss}, were performed with the same specimen (e.g. for the alloys with $x = 0.54$, 0.62 (WQZP) and $x = 0.48$ (SCA)). Some samples were exposed to air (10^5 Pa) and to a low air pressure (10^{-3} Pa), but no effect of oxidation was observed by XRD. Two or three experiments were performed with each alloy and reproducible results were obtained. Appropriate precautions were undertaken in order to minimize systematic aberrations which could influence the observed values of the unit-cell parameters of the phases α, α', α_{ss} and β(Zn) [7,8].

3. Results and discussion

In line with the phase diagram accepted in the literature, one could expect the following phase transitions:

(i) for the alloys with $x = 0.44$, 0.48 and 0.54,

$$\alpha(\mathrm{M}/\beta) + \beta(\mathrm{Zn}) \rightleftharpoons \alpha' + \alpha(\mathrm{M}/\alpha') \rightleftharpoons \alpha_{\mathrm{ss}},$$

(ii) for the alloys with $x = 0.62$,

$$\alpha(\mathrm{M}/\beta) + \beta(\mathrm{Zn}) \rightleftharpoons \alpha' + \beta(\mathrm{Zn}) \rightleftharpoons \alpha_{\mathrm{ss}}.$$

However, the following sequence of phase transitions has been observed for the studied alloys with $x = 0.44$ and 0.48 (in which Al is dominant) (Ref. [6] and the present work)

$$\alpha(\mathrm{M}/\beta) + \beta(\mathrm{Zn}) \rightleftharpoons \alpha' + \beta(\mathrm{Zn}) + \alpha(\mathrm{M}/\alpha', \beta) \rightleftharpoons \alpha_{\mathrm{ss}}.$$

On the other hand, for the studied alloys having $x = 0.54$ and 0.62 (in which Zn is dominant), the following phase transitions have been observed [4]

$$\alpha(\mathrm{M}/\beta) + \beta(\mathrm{Zn}) \rightleftharpoons \alpha' + \beta(\mathrm{Zn}) + \alpha(\mathrm{M}/\alpha', \beta) \rightleftharpoons \alpha' + \beta(\mathrm{Zn}) \rightleftharpoons \alpha_{\mathrm{ss}}.$$

These results indicate that a correction in the phase diagram of the system Al–Zn is necessary.

Our previous and present studies have shown that the unit-cell parameter of the $\alpha(\mathrm{M}/\beta)$-phase, in equilibrium with the β(Zn)-phase approached after a prolonged ageing of the quenched alloy, does not depend on the initial composition, amounting

0.40469(6) nm at RT. On the other hand, the unit-cell parameter of the α(M/β)-phase of the alloy approaching the equilibrium state by slow cooling from T_{ss} to RT and by ageing at RT, is 0.40445(10) nm, regardless of the initial composition (Ref. [3] and references therein, Refs. [4,6], the present work). That difference between the two values of the unit-cell parameter is due to different content of Zn retained in the matrix, as a result of different thermal treatments. For comparison, the unit-cell parameter of pure Al amounts 0.40494(3) nm [3].

From Refs. [3,4,6] and the present work it follows that the unit-cell parameters of the β(Zn)-phase, in equilibrium with the α(M/β)-phase, are close to those of pure Zn at RT, namely, a = 0.2665(2) nm, c = 0.4947(3) nm (space group $P6_3/mmc$). The above cited values have been used to calibrate the angular scale in high-temperature XRD measurements in the previous works [4,6] and in the present work.

The figures given in the present work correspond to the alloys, quenched from T_{ss} to RT and aged at RT for 11 months (samples WQAP). Figure 1 shows prominent diffraction line profiles (scanned *in situ*) at medium Bragg angles, of the alloy with

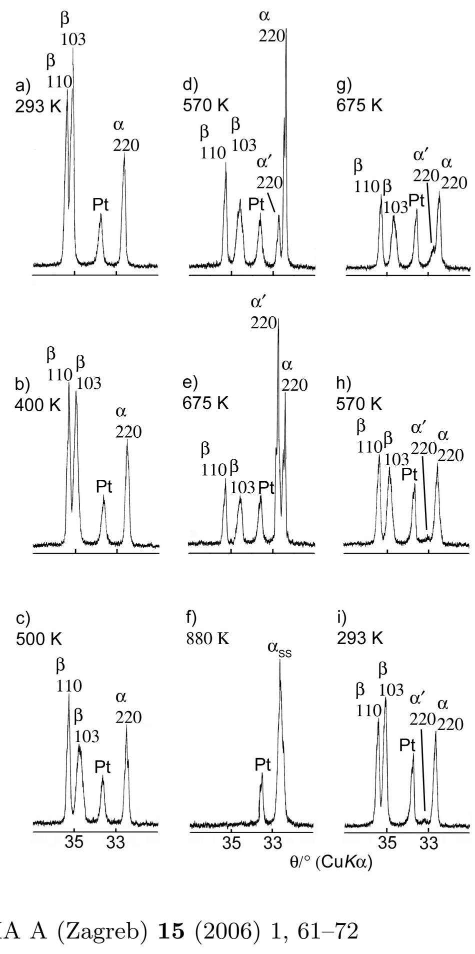

Fig. 1. Prominent diffraction lines of the alloy Al-44 at % Zn at selected temperatures. The alloy was quenched from the solid-solution temperature, T_{ss}, to RT (in water) and aged at RT for 11 months. Radiation: monochromatized (graphite) Cu$K\alpha$, counter: proportional.

$x = 0.44$ at selected temperatures, including the heating run and the cooling run. Figure 2 shows the temperature dependence of the unit-cell parameter a of the phases α, α' and α_{ss} of the alloy with $x = 0.44$, during the heating and cooling runs. The direction of temperature change is shown by arrows, and vertical bars indicate the estimated standard deviation (e.s.d.) in the derived parameter values. The same features are also given in the following figures. The temperature dependence of the unit-cell parameters $a(\beta)$ and $c(\beta)$ of the β(Zn)-phase is shown in Figs. 3

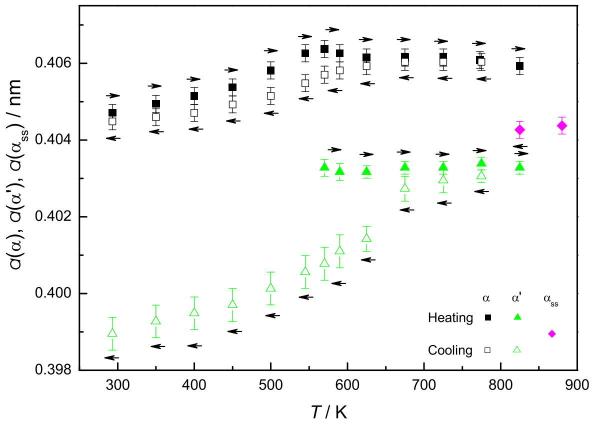

Fig. 2. The dependence of the unit-cell parameter, a, of the phases α, α' and α_{ss} in the water-quenched alloy Al-44 *at* % Zn *(aged at RT for 11 months) on temperature during heating from RT to T_{ss} and cooling to RT. The arrows indicate the direction of temperature change. Vertical bars indicate the estimated standard deviation (e.s.d.) of a.*

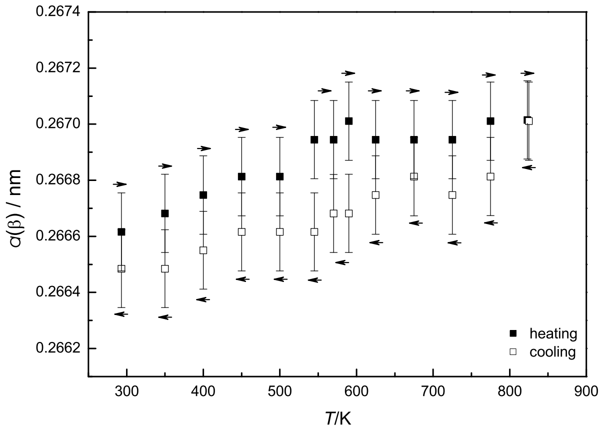

Fig. 3. The dependence of the unit-cell parameter $a(\beta)$ of the phase β(Zn) *in the water-quenched alloy* Al-44 *at* % Zn *(aged at RT for 11 months) on temperature during heating from RT to T_{ss} and cooling to RT. The arrows indicate the direction of temperature change. Vertical bars indicate e.s.d. of $a(\beta)$.*

and 4, respectively, for the alloy with $x = 0.44$. Figure 5 shows the temperature dependence of an interplanar spacing of the β(Zn)-phase, namely d_{103} (which is of a particular interest, including both the temperature behaviour of the a and c axes) in the alloy with $x = 0.44$. Finally, the temperature change of diffraction line intensities of diffraction lines $\beta 110$ and $\beta 103$ for the alloy with $x = 0.48$ is shown

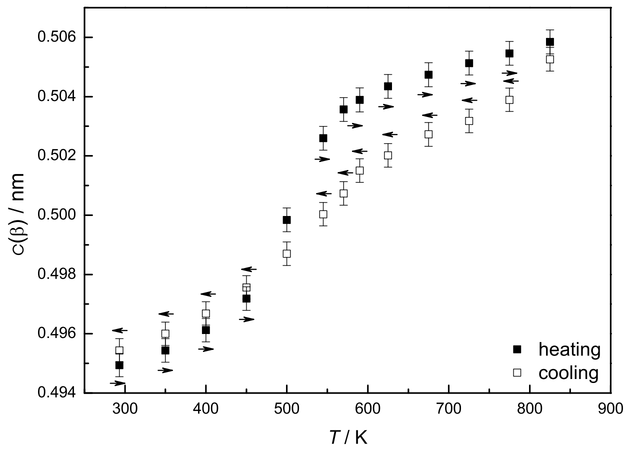

Fig. 4. The dependence of the unit-cell parameter $c(\beta)$ of the phase β(Zn) in the water-quenched alloy Al-44 *at* % Zn *(aged at RT for 11 months) on temperature during heating from RT to T_{ss} and cooling to RT. The arrows indicate the direction of temperature change. Vertical bars indicate e.s.d. in $c(\beta)$.*

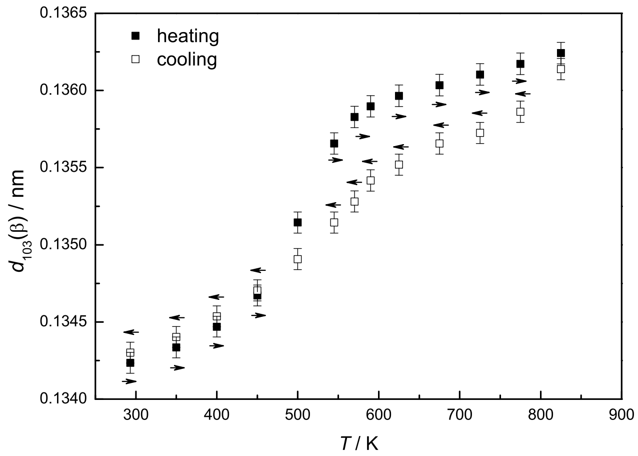

Fig. 5. The dependence of the interplanar spacing d_{103} of the phase β(Zn) in the water-quenched alloy Al-44 *at* % Zn *(aged at RT for eleven months) on temperature during heating from RT to T_{ss} and cooling to RT. The arrows indicate the direction of temperature change. Vertical bars indicate e.s.d. of d_{103}.*

in Fig. 6. Similar figures showing the temperature dependence of microstructure of the alloys in the Zn-rich region (water-quenched from T_{ss} to RT and prolonged aged at RT, WQZP) and in the Al-rich region (water-quenched/slowly cooled from T_{ss} to RT and aged for one/two week(s) at RT, WQA, SCA) are given in the previous articles [4, 6].

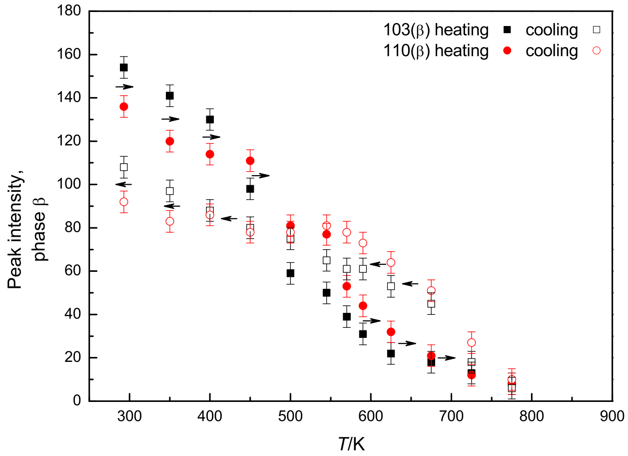

Fig. 6. The dependence of peak intensities (arbitrary units) of diffraction lines 110 and 103 of the phase β*(Zn) on temperature for the alloy* Al-48 *at%* Zn *during heating and cooling cycle. The alloy was water quenched from* T_{ss} *to RT and aged at RT for 11 months. The arrows indicate the direction of temperature change. Vertical bars indicate e.s.d. of peak intensity.*

General features of the temperature dependence of XRD patterns, and therefore, of their microstructure, of the studied alloys are as follows. By comparison of the water-quenched alloys (WQZP, WQA, WQAP) with the slowly-cooled alloys (SCA), one can conclude that the temperature dependence of their microstructure is rather different, e.g. Ref. [6], Figs. 2, 4, 6 *vs.* Figs. 3, 5, 7. The two curves, which show this dependence during the first heating from RT to T_{ss} and cooling from T_{ss} to RT, are closer to each other for the slowly-cooled samples than for the water-quenched samples. That is, the area between these two curves is smaller for the slowly-cooled samples than for the water-quenched samples. That area slightly increases with the increase of the Zn content, x, in the alloys. For the water-quenched samples, the curves corresponding to the second heating from RT to T_{ss} and second cooling from T_{ss} to RT are close to the one of the first cooling from T_{ss} to RT; these curves can be approximated by a linear function, e.g. Ref. [4], Figs. 2, 3, 5; Ref. [6], Figs. 4, 6; the present work, Figs. 3 – 5. On the contrary, the curve corresponding to the first heating from RT to T_{ss} is quite different, deviating much from the linear function. Generally, at a given temperature, the difference between the values of a microstructural parameter, found in the heating run and in the cooling run, is smaller for the slowly-cooled samples than for the water-quenched samples, this difference slightly decreases with the prolonged ageing of one and the same alloy (e.g. samples WQAP *vs.* samples WQA).

As the temperature of the alloy increases, a decrease of the diffraction line intensities of both α(M/β)- and β(Zn)-phases takes place, due to enhanced thermal vibrations of the atoms. A gradual shift of the diffraction lines toward smaller Bragg angles is observed, caused by thermal expansion (Fig. 1 in Refs. [4,6], the present work). Thermal expansion of the β(Zn)-phase is anisotropic. It can be followed, e.g. from the temperature dependence of the angular separation of adjacent diffraction lines, β110 and β103 (Fig. 1 in Refs. [4,6], the present work). Thermal expansion along the c-axis is several times bigger than that along the a-axis of the β(Zn)-phase (Table 1 in Ref. [4]). An indication of the thermal expansion anisotropy may also be a decrease of the saddle intensity between the adjacent diffraction lines β110 and β103 as the temperature increases (Fig. 1 in Refs. [4,6], the present work). For the studied alloys (Refs. [4,6], the present work) one can also observe a change of the shape of the β(Zn)-precipitates with the increase of the temperature: the broadening of diffraction lines with $l \neq 0$ (e.g. β002, β103) increases in relation to broadening of diffraction lines with $l = 0$ (e.g. β100, β110). β(Zn)-precipitates become more and more flat, i.e. their size along the c-axis decreases as the temperature increases. Zn atoms, which leave the β(Zn)-precipitates, are dominantly those which form the lattice planes $\beta\{001\}$. This effect was not observed for the alloys with smaller Zn content ($x \leq 0.40$, Ref. [3]). It may be supposed that the concentration of vacancies in the β(Zn)-phase increases with temperature; this affects the temperature dependence of its a- and c-unit cell parameters for the water-quenched alloys (Ref. [4] (WQZP), Figs. 3 – 5; Ref. [6] (WQA), Figs. 4, 6; the present work (WQAP), Figs. 3 – 5).

For the water-quenched and slowly-cooled alloys, the unit-cell parameter, a, of the α(M/β)-phase changes rather linearly during the first heating run up to ≈ 500 K (Ref. [4], Fig. 2; Ref. [6], Figs. 2, 3; the present work, Fig. 2). At a higher temperature, a partial dissolution of Zn from β(Zn)-phase into the α(M/β)-phase is observed. This process compensates and even reverses the change of the unit-cell parameter a of the α(M/β)-phase due to thermal expansion, as the Zn atoms are smaller than the Al atoms (Ref. [4], Fig. 2; Ref. [6], Figs. 2, 3; the present work, Fig. 2).

Above ≈ 550 K a new phase, α' (fcc), appears in accordance with the phase diagram [1,2]. The unit-cell parameter of the α'-phase, being rich with Zn, is smaller (0.8 to 0.9 % at 560 K) than the one of the α-phase. Therefore, diffraction lines of the α'-phase are at the high-angle side of diffraction lines (having the same Miller indices) of the α-phase. In line with the phase diagram, for the alloys with $x = 0.44$, 0.48, and 0.54, the α-phase should be in coexistence with the α'-phase above ≈ 550 K, i.e. the β(Zn)-phase should completely transform into the α'-phase above that temperature. On the other hand, for the alloy with $x = 0.62$, the phases α' and β(Zn) should be present above ≈ 550 K. However, our previous [4,6] and present results indicate that only a partial transition of the β(Zn)-phase, and probably a partial transition of the α(M/β)-phase, into the α' (fcc)-phase takes place above ≈ 550 K. It follows that the α-phase is in coexistence with both α'- and β(Zn)-phases, and it is now denoted as α(M/α', β). As the temperature further increases, the composition of the phases changes, the content of Zn in the $\alpha(\mathrm{M}/\alpha', \beta)$-phase, and probably in the α'-phase, increases. These Zn atoms come from the β(Zn)-phase, in which the concentration of vacancies increases; this effect compensates thermal expansion of the β(Zn)-phase (Ref. [4], Figs. 4, 5; Ref. [6], Figs. 4, 6; the present work, Figs. 3 – 5). For the slowly-cooled alloys, the concentration of vacancies above $\approx$ 550 K is obviously smaller than in the water-quenched alloys, as the influence on thermal expansion is small (Ref. [6], Figs. 5, 7). Diffraction line intensities of the α'-phase increase, while those of β(Zn)-phase and $\alpha(\mathrm{M}/\alpha', \beta)$-phase decrease.

Figure 6 shows the temperature dependence of the peak intensities of diffraction lines 110(β) and 103(β). One can notice three intervals in this dependence: first, a decrease of intensity due to enhanced thermal vibrations of atoms; second (above $\approx$ 500 K), a steeper decrease due to dissolution of Zn atoms from the β(Zn)-phase into the $\alpha(\mathrm{M}/\beta)$-phase; third (above $\approx$ 600 K), a slower decrease toward the formation of solid solution.

For the alloys with $x = 0.44$ and 0.48, the solid solution, α_{ss} (fcc), is formed at $\approx$ 880 K for the water-quenched samples (WQA, WQAP), and at $\approx$ 720 K for the SCA samples (Ref. [6], the present work).

However, for the alloys with $x = 0.54$ and 0.62 (WQZP), the $\alpha(\mathrm{M}/\alpha', \beta)$-phase disappears at about $\approx$ 650 K in the first heating run, the α'-phase remaining in coexistence with the β(Zn)-phase. Solid solution, α_{ss} (fcc), is formed at $\approx$ 700 K. In the first cooling run from T_{ss} to RT, a temperature hysteresis in reversal phase transitions is observed (Ref. [4], Figs. 2, 3). In the repeated, second, heating run of the same specimen a temperature delay in phase transitions of several tens of K is found in relation to the first heating run (Ref. [4], Figs. 3 – 5). The $\alpha(\mathrm{M}/\alpha', \beta)$-phase disappears at $\approx$ 720 K and the solid solution, α_{ss} (fcc) is formed at $\approx$ 800 K. During the second cooling run, the microstructural parameters show a similar dependence on temperature as in the first cooling run and in the second heating run (Ref. [4], Figs. 2b, 3).

A similar behaviour during the first cooling run is observed for the alloys with $x = 0.44$ and 0.48 (WQA, WQAP). The intensity of diffraction lines of the α'-phase decreases during cooling more rapidly than it increases during the heating, i.e. at a given temperature the intensity is smaller in the cooling run than in the heating run (Ref. [6], Fig. 1; the present work, Fig. 1). The opposite is observed for the β(Zn)-phase (Ref. [6], Fig. 1, the present work, Fig. 1). This is also shown in Fig. 6: the temperature behaviour of the peak intensities of diffraction lines of the β(Zn)-phase is different in the first cooling run from that in the first heating run.

4. *Conclusion*

It has been shown in the previous works (Refs. [4,6]) and in the present work that the temperature dependence of the microstructure of the studied Al–Zn alloys is strongly governed by the previous thermal treatments. The alloys containing 44, 48, 54 and 62 at% Zn were rapidly quenched from the solid-solution temperature

(T_{ss}) in water to RT and aged at RT for one (two) week(s) (WQA) or for 11 months (WQAP, WQZP). The alloys were also slowly cooled from T_{ss} to RT and aged at RT (SCA). The different behaviour of water-quenched *vs.* slowly-cooled alloys during the temperature change follows from their different starting microstructure prior to examination by XRD. One may suppose that the SCA alloys are much closer to the equilibrium state than are the WQA/WQAP/WQZP alloys. In the WQA/WQAP/WQZP alloys, the precipitates β(Zn) are not uniformly distributed in the crystal lattice of the $\alpha(M/\beta)$-phase, and residual strains in the $\alpha(M/\beta)$-phase around the β(Zn)-precipitates are present. This fact was proved in detail by accurate XRD measurements in Ref. [3]. A very important point is that quenched-in vacancies at RT are much more numerous in the WQA/WQAP/WQZP alloys than in the SCA alloys. The first heating run of the WQA/WQAP/WQZP alloys was slow, at a rate of 2 to 3 K/min; the alloys were held for $\approx$ 15 minutes at a series of temperatures during scanning of diffraction pattern. The first cooling run was performed in a similar way. Therefore, most of strains in the WQA/WQAP/WQZP alloys were annealed after completing the first heating and cooling runs. The resulting microstructure at RT was different from the starting microstructure at RT, concerning the size and shape of the β(Zn)-precipitates, their distribution in the crystal lattice in the $\alpha(M/\beta)$-phase, and lattice strains around the precipitates. The vacancies were obviously much less numerous than in the starting quenched alloys. One has to keep in mind that vacancies play a dominant role in the diffusion rate of Zn atoms; this may explain the delay in phase transitions during the second heating run in relation to the first heating run.

The temperature behaviour of the slowly-cooled alloys is rather different from that of the quenched alloys. A prolonged ageing of the quenched alloys (up to 11 months) has little influence on the temperature behaviour of the alloys. The ideal equilibrium state cannot be reached either by slow cooling from T_{ss} to RT over several days, or by prolonged ageing at RT of the rapidly quenched alloys.

References

[1] H. Löffler, *Structure and Structure Development in Al–Zn Alloys*, Akademie Verlag, Berlin (1995).

[2] H. Löffler, G. Wendrock and O. Simmich, phys. stat. sol. (a) **132** (1992) 339.

[3] S. Popović and B. Gržeta, Croat. Chem. Acta **72** (1999) 621, and references therein.

[4] S. Popović, B. Gržeta, B. Hanžek and S. Hajster, Fizika A (Zagreb) **8** (1999) 173.

[5] S. Popović and B. Gržeta, Mater. Sci. Forum **321-324** (2000) 635.

[6] Ž. Skoko and S. Popović, Fizika A (Zagreb) **10** (2001) 191.

[7] S. Popović, J. Appl. Cryst. **4** (1971) 240; **6** (1973) 122.

[8] S. Popović, Cryst. Res. Technol. **20** (1985) 552.

TEMPERATURNA OVISNOST MIKROSTRUKTURE SLITINA $(1-x)$Al–xZn, $x = 0.44$, 0.48, 0.54 I 0.62

Istraživali smo ovisnost mikrostrukture navedenih slitina o temperaturi *in situ* pomoću rentgenske difrakcije u prahu. Pokazali smo da je temperaturna ovisnost mikrostrukture slitina, brzo kaljenih s temperature čvrste otopine, T_{ss}, na sobnu temperaturu, RT, bitno različita od one za slitine, koje su sporo hlađene s T_{ss} na RT. Površina između dviju krivulja, koje pokazuju tu ovisnost tijekom prvog grijanja slitine od RT do T_{ss} i prvog hlađenja od T_{ss} do RT, mnogo je manja za sporo hlađene slitine nego za brzo kaljene slitine. Ta površina lagano raste s udjelom Zn u slitinama. Temperaturna ovisnost mikrostrukture slitina tijekom drugog grijanja od RT do T_{ss} i drugog hlađenja od T_{ss} do RT malo se razlikuje od ovisnosti tijekom prvog hlađenja od T_{ss} do RT. Idealno ravnotežno stanje ne može se postići niti sporim hlađenjem slitina od T_{ss} do RT niti dugim starenjem pri RT slitina brzo kaljenih od T_{ss} na RT. Opaženi niz faznih pretvorbi u slitinama tijekom grijanja od RT do T_{ss} razlikuje se od onoga koji bi se očekivao prema faznom dijagramu sustava Al–Zn, prihvaćnog u literaturi. Tijekom hlađenja slitine od T_{ss} do RT uočili smo temperaturnu histerezu za obrnute fazne pretvorbe.